

Mesoscopic conductance fluctuations in graphene samples

Maxim Yu. Kharitonov¹ and Konstantin B. Efetov^{1,2}

¹ *Theoretische Physik III, Ruhr-Universität Bochum, Germany*

² *L.D. Landau Institute for Theoretical Physics, Moscow, Russia*

(Dated: November 2, 2018)

Mesoscopic conductance fluctuations in graphene samples at energies not very close to the Dirac point are studied analytically. We demonstrate that the conductance variance $\langle [\delta G]^2 \rangle$ is very sensitive to the elastic scattering breaking the valley symmetry. In the absence of such scattering (disorder potential smooth at atomic scales, trigonal warping negligible), the variance $\langle [\delta G]^2 \rangle = 4\langle [\delta G]^2 \rangle_{\text{metal}}$ is four times greater than that in conventional metals, which is due to the two-fold valley degeneracy. In the absence of intervalley scattering, but for strong intravalley scattering and/or strong warping $\langle [\delta G]^2 \rangle = 2\langle [\delta G]^2 \rangle_{\text{metal}}$. Only in the limit of strong intervalley scattering $\langle [\delta G]^2 \rangle = \langle [\delta G]^2 \rangle_{\text{metal}}$. Our theory explains recent numerical results and can be used for comparison with existing experiments.

PACS numbers: 73.63.-b, 72.15.Rn, 81.05.Uw

Introduction. Graphene (a monolayer of graphite) is a novel material [1, 2, 3, 4] with the Dirac electronic spectrum. A lot of progress in the theoretical understanding of clean graphene has been made so far (see e.g. Ref. [5]). For many interesting effects, however, disorder plays a significant role. A peculiar feature of disordered graphene is that its physical properties are sensitive to the scattering processes breaking the valley symmetry.

This sensitivity has been revealed in the behavior of the weak localization (WL) correction to conductivity [6, 7, 8, 9, 10]. Another famous phenomenon due to disorder that goes along with WL are the mesoscopic conductance fluctuations (CF). CF with variance $\sim e^2/\hbar$ are observed in graphene samples experimentally [4, 11, 12, 13], although a detailed analysis has not been reported.

Numerical investigation of CF in graphene has been undertaken recently in Ref. [14]. The authors have rather unexpectedly found that CF in graphene were considerably stronger than those in conventional metals [15, 16] and the variance did not seem to be universal. No clear explanation of this effect was given in Ref. [14], although it was argued that the unusual behavior might be due to percolation effects.

Here we develop an analytical theory of conductance fluctuations in diffusive graphene samples at energies not very close to the Dirac point. The results we obtain explain the findings of Ref. [14] and can be directly used for comparison with the experiments.

Model. We consider a general microscopic model of disorder in graphene. The single-particle Hamiltonian of the system is (we put $\hbar = 1$ and recover it later on)

$$\hat{H}_{\mathbf{r}} = \hat{H}_0 + \hat{H}_w + \hat{V}(\mathbf{r}), \quad \hat{H}_0 = -iv(1^{KK'} \otimes \tau_{\lambda}^{AB})\partial_{\lambda}. \quad (1)$$

Here $\hat{H}_w = \mu_w \tau_z^{KK'} \otimes [\tau_x(\partial_x^2 - \partial_y^2) - 2\tau_y \partial_x \partial_y]^{AB}$ describes weak trigonal warping and $\lambda = x, y$. The Hamiltonian $\hat{H}_{\mathbf{r}}$ is a matrix in the tensor product $KK' \otimes AB$ of the valley (KK') and sub-lattice (AB) spaces and $1, \tau_{x,y,z}$ are the unity and Pauli matrices. The random disorder potential

$\hat{V}(\mathbf{r})$ is Gaussian with the correlation function

$$\langle \hat{V}(\mathbf{r}) \otimes \hat{V}(\mathbf{r}') \rangle = \{ \Lambda_0 \mathbb{1} \otimes \mathbb{1} + \Lambda_l^k \mathcal{T}_{kl} \otimes \mathcal{T}_{kl} \} \delta(\mathbf{r} - \mathbf{r}'), \quad (2)$$

where $\mathbb{1} = 1^{KK'} \otimes 1^{AB}$, $\mathcal{T}_{kl} = \tau_k^{KK'} \otimes \tau_l^{AB}$, $k, l = x, y, z$. For a given Fermi energy ϵ the scattering rates (inverse scattering times) are defined as

$$(\gamma_0, \gamma_{zz}, \gamma_{z\perp}, \gamma_{\perp z}, \gamma_{\perp\perp}) \equiv \pi\nu(\Lambda_0, \Lambda_z^z, \Lambda_{x,y}^z, \Lambda_z^{x,y}, \Lambda_{x,y}^{x,y}),$$

where $\nu = \epsilon/(2\pi v^2)$ is the density of states per one valley and one spin.

In Eq. (2), the term $\propto \gamma_0$ arises from remote charge impurities in the substrate, the field of which varies smoothly at atomic scales, while the rest of the terms describe various atomically-sharp defects that break the valley symmetry. Being diagonal in KK' -space ($\propto \tau_z^{KK'}$), the terms $\propto \gamma_{zz}$ and $\propto \gamma_{z\perp}$ do not involve the intervalley scattering, but do lift the valley degeneracy by acting differently on the valleys. Such terms describe the intravalley scattering, whereas the terms $\propto \gamma_{\perp z}$ and $\propto \gamma_{\perp\perp}$ are due to

Calculations. We calculate the correlation function

$$F_{\alpha\beta, \gamma\delta}(\Delta\epsilon, H, \Delta H) = \langle \delta\sigma_{\alpha\beta}(\epsilon + \Delta\epsilon, H + \Delta H) \delta\sigma_{\gamma\delta}(\epsilon, H) \rangle \quad (3)$$

of the conductivities $\sigma_{\alpha\beta}(\epsilon + \Delta\epsilon, H + \Delta H)$ and $\sigma_{\gamma\delta}(\epsilon, H)$ taken at the Fermi energies $\epsilon + \Delta\epsilon, \epsilon$ [17] and magnetic fields $H + \Delta H, H$ ($\alpha, \beta, \gamma, \delta = x, y$ and $\delta\sigma = \sigma - \langle \sigma \rangle$).

We use the averaging technique developed for conventional disordered metals [18]. We assume (i) weak disorder, $\Lambda_0/v^2 \ll 1$, and (ii) diffusive regime, i.e., that the mean free path $l = v/\gamma_0$ is much smaller than the size of the sample and the valley-symmetric rate γ_0 is dominant, $\gamma_0 \gg \gamma_{\{z,\perp\},\{z,\perp\}}$. As it was shown in Ref. [9] one should first renormalize the velocity v and constants Λ [Eq. (2)] solving renormalization group equations and then use them for calculating the localization corrections. This procedure is valid so long as $\epsilon \gtrsim \epsilon_0 \exp(-\pi v^2/\Lambda_0)$, where ϵ_0 is an atomic-scale energy. The same can be done for the correlation function (3) and we further assume that

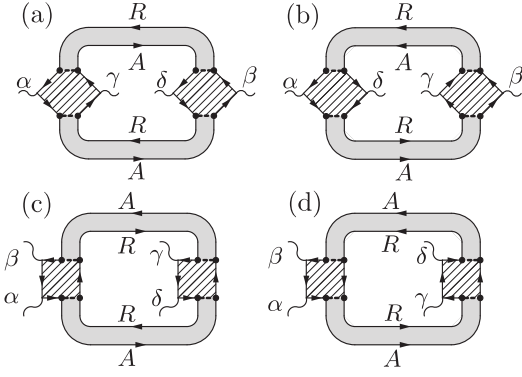


FIG. 1: Diagrams for the conductivity correlation function $F_{\alpha\beta,\gamma\delta}(\Delta\epsilon, H, \Delta H)$ [Eq. (10)]. Gray stripes denote diffusons and Cooperons, rendered with lines blocks are Hikami boxes, see Fig. 2. The diagrams (c),(d) with the substitution $\alpha \leftrightarrow \beta$, $\gamma \leftrightarrow \delta$, $R \leftrightarrow A$ must also be considered.

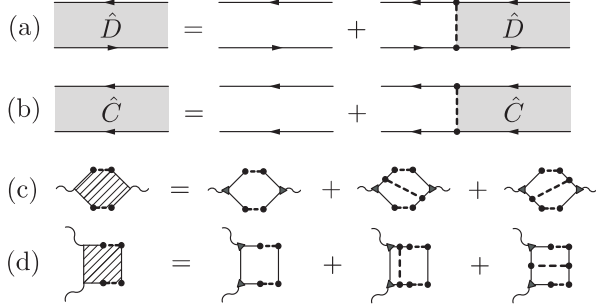


FIG. 2: (a),(b) Diagrammatic representation of the integral equations for the diffuson and Cooperon. (c),(d) Hikami boxes. The current vertex renormalized by disorder (dark triangle) equals $\tilde{j}_\alpha = 2ev(1^{KK'} \otimes \tau_\alpha^{AB})$.

v and Λ 's have been renormalized. Under these assumptions, the calculations for graphene generalize those for ordinary metals [15, 16] and $F_{\alpha\beta,\gamma\delta}(\Delta\epsilon, H, \Delta H)$ is given

$$\hat{D}_\omega(\mathbf{r}, \mathbf{r}') = \frac{\pi\nu}{16} \{ [D_\omega^0 + D_\omega^1 + 2D_\omega^{2,3}] 1 \otimes 1 + [D_\omega^0 + D_\omega^1 - 2D_\omega^{2,3}] \tau_z \otimes \tau_z + [D_\omega^0 - D_\omega^1] \tau_\lambda \otimes \tau_\lambda \} \otimes (1 \otimes 1 + \tau_k \otimes \tau_k) \quad (6)$$

$$\hat{C}_\omega(\mathbf{r}, \mathbf{r}') = \frac{\pi\nu}{16} \{ [2C_\omega^{2,3} + C_\omega^1 + C_\omega^0] 1 \otimes 1 + [2C_\omega^{2,3} - C_\omega^1 - C_\omega^0] \tau_z \otimes \tau_z + [C_\omega^1 - C_\omega^0] \tau_\lambda \otimes \tau_\lambda \} \otimes (1 \otimes 1 - \tau_k \otimes \tau_k) \quad (7)$$

In Eqs. (6) and (7), the tensor products are ordered as $(R \otimes A)_{KK'} \otimes (R \otimes A)_{AB}$, $\lambda = x, y$, and $k = x, y, z$. The diffuson/Cooperon components $D_\omega^i = D_\omega^i(\mathbf{r}, \mathbf{r}')$ and $C_\omega^i = C_\omega^i(\mathbf{r}, \mathbf{r}')$, $i = 0, 1, 2, 3$, satisfy the equations

$$\{-i\omega - D\nabla_{D,C}^2 + \Gamma_i + \gamma_{\text{inel}}\}(D, C)_\omega^i(\mathbf{r}, \mathbf{r}') = \delta(\mathbf{r} - \mathbf{r}'), \quad (8)$$

where $\nabla_D = \nabla - i(e/c)\Delta\mathbf{A}(\mathbf{r})$, $\nabla_C = \nabla - i(e/c)[2\mathbf{A}(\mathbf{r}) + \Delta\mathbf{A}(\mathbf{r})]$, the vector potentials $\mathbf{A}(\mathbf{r})$, $\Delta\mathbf{A}(\mathbf{r})$ correspond to H and ΔH , respectively, $D = v^2/\gamma_0$ is the diffusion

coefficient, and γ_{inel} is the inelastic scattering rate due to, e.g., electron-electron or electron-phonon interactions. The elastic scattering rates Γ_i due to disorder equal

$$\Gamma_0 = 0, \quad \Gamma_1 = 4\gamma_\perp, \quad \Gamma_2 = \Gamma_3 = 2\gamma_\perp + 2\gamma_z + 2\gamma_w, \quad (9)$$

where the total intervalley $\gamma_\perp = \gamma_{\perp z} + 2\gamma_{\perp\perp}$ and intravalley $\gamma_z = \gamma_{zz} + 2\gamma_{z\perp}$ scattering rates were introduced.

The Cooperon in the form of Eq. (7) has been obtained earlier [7, 9], whereas the form (6) of the diffuson is ob-

by the diagrams in Fig. 1. The arising disorder-averaged products of the exact retarded (R) and advanced (A) Green's functions $\hat{\mathcal{G}}^{R,A}$ yield the diffusons and Cooperons defined as:

$$\hat{D}_\omega(\mathbf{r}, \mathbf{r}') \equiv \langle \hat{\mathcal{G}}^R(\epsilon + \omega, \mathbf{r}, \mathbf{r}') \otimes \hat{\mathcal{G}}^A(\epsilon, \mathbf{r}', \mathbf{r}) \rangle, \quad (4)$$

$$\hat{C}_\omega(\mathbf{r}, \mathbf{r}') \equiv \langle \hat{\mathcal{G}}^R(\epsilon + \omega, \mathbf{r}, \mathbf{r}') \otimes \hat{\mathcal{G}}^A(\epsilon, \mathbf{r}, \mathbf{r}') \rangle. \quad (5)$$

They satisfy the integral equations represented diagrammatically in Fig. 2(a),(b). These equations possess a non-trivial matrix structure acquired from the correlator (2) (dashed lines) and disorder-averaged ($\hat{\mathcal{G}}^{R,A}$) (fermionic lines). Consequently, there exist ‘‘high-energy’’ modes of \hat{D} and \hat{C} with gaps $\sim \gamma_0$ as well as ‘‘low-energy’’ modes, which gaps do not contain γ_0 [7, 9]. Giving much greater contribution in the diffusive regime, only the latter low-energy modes are of interest here.

The effect of trigonal warping can be taken into account in $\hat{\mathcal{G}}^{R,A}$ up to the second order in \hat{H}_w . As a result, the self-energies of the Green's functions ($\hat{\mathcal{G}}^{R,A}$) acquire the warping rate $\gamma_w = (\mu_w \epsilon / v^2)^2 / \gamma_0$ and the dashed line in Fig. 2(a),(b), in addition to the correlator (2), also represents the ‘‘warping term’’

$$\hat{\gamma}_w^{D,C} = \pm \gamma_w (\tau_z^{KK'} \otimes 1^{AB})_R \otimes (\tau_z^{KK'} \otimes 1^{AB})_A$$

with + and - for the diffuson [D,(a)] and Cooperon [C,(b)], respectively. It appears that, in the *low-energy* diffuson/Cooperon subspaces, the matrix structure of the warping term $\hat{\gamma}_w^{D,C}$ is *identical* to that of the intravalley scattering of type $\hat{\gamma}_{zz} = \gamma_{zz} \mathcal{T}_{zz} \otimes \mathcal{T}_{zz}$ in Eq. (2). Therefore, the effect of warping on the low-energy diffusion modes of \hat{D} and \hat{C} is not any different from that of the intravalley scattering $\propto \gamma_{zz}$ and the effect of warping could be taken into account by the substitution $\gamma_{zz} \rightarrow \gamma_{zz} + \gamma_w$.

Resolving the matrix-structure of the equations in Fig. 2(a),(b), we obtain:

tained here for the first time. Note that for a given i the rates Γ_i [Eq. (9)] entering the corresponding diffuson D_ω^i and Cooperon C_ω^i modes are identical. The fact that the insensitive to various phase-breaking phenomena diffuson \hat{D} does contain the rates γ_z , γ_\perp , and γ_w [19] means that

$$F_{\alpha\beta,\gamma\delta}(\Delta\epsilon, H, \Delta H) = \langle \delta\sigma_{\alpha\beta}(\epsilon + \Delta\epsilon, H + \Delta H) \delta\sigma_{\gamma\delta}(\epsilon, H) \rangle = (2_s 2_v e^2 D)^2 \int \frac{d\epsilon d\epsilon'}{(2\pi)^2} \frac{dn(\epsilon)}{d\epsilon} \frac{dn(\epsilon')}{d\epsilon'} \frac{1}{\mathcal{S}} \\ \times \int d\mathbf{r} d\mathbf{r}' \sum_{i=0}^3 \left\{ \delta_{\alpha\gamma} \delta_{\beta\delta} |D_\omega^i(\mathbf{r}, \mathbf{r}')|^2 + \delta_{\alpha\delta} \delta_{\beta\gamma} |C_\omega^i(\mathbf{r}, \mathbf{r}')|^2 + \frac{1}{2} \delta_{\alpha\beta} \delta_{\gamma\delta} \text{Re}[D_\omega^i(\mathbf{r}, \mathbf{r}') D_\omega^i(\mathbf{r}', \mathbf{r}) + C_\omega^i(\mathbf{r}, \mathbf{r}') C_\omega^i(\mathbf{r}', \mathbf{r})] \right\}, \quad (10)$$

where $\omega = \epsilon - \epsilon' + \Delta\epsilon$, \mathcal{S} is the sample area, $n(\epsilon) = 1/[\exp(\epsilon/T) + 1]$ is the Fermi distribution function, and the factors 2_s and 2_v originate from the dimensionality of the spin and valley spaces (the indices s and v emphasize their origin).

Equation (10), together with Eqs. (6)-(9), constitutes the main result of our work. The key feature characterizing graphene is that different diffuson and Cooperon modes i enter Eq. (10). The magnitude of mesoscopic fluctuations is thus determined by the strength of elastic scattering processes breaking the valley symmetry. When all such effects are negligible, the result (10) for graphene is $(2_v)^2 = 4$ times greater than that for conventional metals [15, 16] due to the two-fold valley degeneracy. Note that at $H = \Delta H = 0$ one has $D_\omega^i = C_\omega^i$ and for a given i the diffuson and Cooperon contribute equally.

To be specific, below we consider the case of a rectangular sample with length \mathcal{L}_x and width \mathcal{L}_y , occupying the area $0 < x < \mathcal{L}_x$, $0 < y < \mathcal{L}_y$, and attached to ideal leads at $x = 0$ and $x = \mathcal{L}_x$. The conductance $G = G_{xx}$ in the x direction is related to the conductivity σ_{xx} as $G = \sigma_{xx} \mathcal{L}_y / \mathcal{L}_x$. From Eq. (10), at $T, \gamma_{\text{inel}} \ll \epsilon_x^*$, where $\epsilon_x^* = \pi^2 D / \mathcal{L}_x^2$ is the Thouless energy for the x dimension, for the *conductance* correlation function $\mathcal{F}(\Delta\epsilon) = \langle \delta G(\epsilon + \Delta\epsilon) \delta G(\epsilon) \rangle = (\mathcal{L}_y / \mathcal{L}_x)^2 F_{xx,xx}(\Delta\epsilon, H, 0)$ we obtain

$$\mathcal{F}(\Delta\epsilon) = \alpha_H \left[\frac{2_s 2_v e^2 D}{2\pi} \right]^2 \frac{1}{\mathcal{L}_x^4} \\ \times \sum_{i=0}^3 \sum_{\mathbf{q}} \left\{ 2 |D_{\Delta\epsilon}^i(\mathbf{q})|^2 + \text{Re}[D_{\Delta\epsilon}^i(\mathbf{q})]^2 \right\}, \quad (11)$$

where $D_{\Delta\epsilon}^i(\mathbf{q}) = 1/(-i\Delta\epsilon + D\mathbf{q}^2 + \Gamma_i)$ are the spatial eigenmodes of the diffuson, $\mathbf{q}^2 = q_x^2 + q_y^2$, $q_x = \pi n_x / \mathcal{L}_x$, $n_x = 1, 2, \dots$, and $q_y = \pi n_y / \mathcal{L}_y$, $n_y = 0, 1, \dots$. In Eq. (11), the factor α_H accounts for the sensitivity of the Cooperons to the magnetic field in the two limiting cases: $\alpha_H = 1$ for $H \ll H^*$ and $\alpha_H = 1/2$ for $H \gg H^*$, where $H^* = (c/e) / \mathcal{L}_x^2$. The conductance vari-

the effects of the intravalley and intervalley scattering and of the trigonal warping should never be understood as a suppression of electron interference alone.

Results. Calculating the diagrams in Fig. 1, for the correlation function of *conductivities* [Eq. (3)] we obtain

ance $\mathcal{F}(\Delta\epsilon = 0) = \langle [\delta G]^2 \rangle$ following from Eq. (11) equals

$$\langle [\delta G]^2 \rangle = 3\alpha_H \left[\frac{2_s 2_v e^2}{2\pi\hbar} \right]^2 \sum_{i=0}^3 \mathcal{R}(\mathcal{L}_i, \mathcal{L}_x, \mathcal{L}_y) \quad (12) \\ \mathcal{R}(\mathcal{L}_i, \mathcal{L}_x, \mathcal{L}_y) = \frac{1}{\pi^4 \mathcal{L}_x^4} \sum_{n_x=1}^{\infty} \sum_{n_y=0}^{\infty} \left[\frac{1}{\mathcal{L}_i^2} + \frac{n_x^2}{\mathcal{L}_x^2} + \frac{n_y^2}{\mathcal{L}_y^2} \right]^{-2} \quad (13)$$

where $\mathcal{L}_i^2 = \pi^2 D / \Gamma_i$. For both narrow ($\mathcal{L}_y \ll \mathcal{L}_x$) and wide ($\mathcal{L}_y \gg \mathcal{L}_x$) samples, the contribution of a given mode i to Eq. (13) is unsuppressed if $\mathcal{L}_i \gg \mathcal{L}_x$ and equals:

$$\mathcal{R}_0 = \mathcal{R}(\infty, \mathcal{L}_x, \mathcal{L}_y) = \begin{cases} 1/90, & \mathcal{L}_y \ll \mathcal{L}_x, \\ \zeta(3) \mathcal{L}_y / (4\pi^3 \mathcal{L}_x), & \mathcal{L}_x \ll \mathcal{L}_y. \end{cases}$$

Wide samples are thus more attractive for the observation of unsuppressed CF. In this case the length \mathcal{L}_i has to be greater than only the shorter dimension \mathcal{L}_x (equivalently, $\Gamma_i \ll \epsilon_x^*$), but can be arbitrary compared to \mathcal{L}_y .

The limiting cases of Eq. (12) for different strengths of the scattering processes can be summarized as follows:

$$\langle [\delta G]^2 \rangle = \frac{2_v^2}{4} \alpha_\gamma \langle [\delta G]^2 \rangle_{\text{m}}, \quad \langle [\delta G]^2 \rangle_{\text{m}} = 12\alpha_H \left[\frac{2_s e^2}{2\pi\hbar} \right]^2 \mathcal{R}_0, \quad (14)$$

where the conductance variance $\langle [\delta G]^2 \rangle_{\text{m}}$ for a conventional metal [15, 16] was introduced. The coefficient α_γ gives the number of diffusion modes i that contribute (i.e., for which $\Gamma_i \ll \epsilon_x^*$) to CF, see Table I. As follows from Eq. (9), the mode $i = 0$ (“pseudo-spin singlet”) is unaffected by any of the scattering mechanisms, the mode $i = 1$ (“triplet, 0”) can be suppressed by the intervalley scattering only, and the modes $i = 2, 3$ (“triplet, ± 1 ”) can be suppressed by both intervalley and intravalley scattering and by trigonal warping. Note that trigonal warping does affect CF, in the same way as intravalley scattering does.

(i) When all the effects are negligible, $\gamma_\perp, \gamma_z, \gamma_w \ll \epsilon_x^*$, all four modes contribute equally, $\alpha_\gamma = 4$, and $\langle [\delta G]^2 \rangle =$

	$\gamma_{\perp} \ll \epsilon_x^*$ and $\gamma_w \ll \epsilon_x^*$	$\gamma_z \gg \epsilon_x^*$ or $\gamma_w \gg \epsilon_x^*$
$\gamma_{\perp} \ll \epsilon_x^*$	4	2
$\gamma_{\perp} \gg \epsilon_x^*$	1	1

TABLE I: The number α_{γ} of the diffusion modes contributing to the conductance variance in graphene for different intervalley γ_{\perp} , intravalley γ_z and trigonal warping γ_w scattering rates. The value of α_{γ} also gives the ratio of the conductance variance in graphene to that in conventional metal, $\langle[\delta G]^2\rangle_{\text{graphene}} = \alpha_{\gamma} \langle[\delta G]^2\rangle_{\text{metal}}$, see Eq. (14).

$4\langle[\delta G]^2\rangle_m$ is four times greater than that for a conventional metal. This is explained by an additional two-fold valley degeneracy described by the factor 2_v in Eq. (14).

(ii) If the intervalley scattering is weak, $\gamma_{\perp} \ll \epsilon_x^*$, but either the intravalley scattering or the trigonal warping are sufficiently strong, $\gamma_z \gg \epsilon_x^*$ or $\gamma_w \gg \epsilon_x^*$, then the two modes $i = 0, 1$ contribute, while the modes $i = 2, 3$ are suppressed. In this case $\alpha_{\gamma} = 2$ and $\langle[\delta G]^2\rangle = 2\langle[\delta G]^2\rangle_m$ is two times greater than that for a metal.

(iii) Finally, if the intervalley scattering is strong, $\gamma_{\perp} \ll \epsilon_x^*$, and the intravalley scattering γ_z and trigonal warping γ_w rates are arbitrary compared to ϵ_x^* , then all triplet modes $i = 1, 2, 3$ are suppressed, and only the gapless mode $i = 0$ contributes. In this case $\alpha_{\gamma} = 1$ and $\langle[\delta G]^2\rangle = \langle[\delta G]^2\rangle_m$ coincides with that for a metal.

The conductances fluctuations in graphene were studied numerically in Ref. [14] (see Fig. 3 therein). For atomically-sharp disorder, a plateau $\langle[\delta G]^2\rangle_{\text{plateau}} \approx \langle[\delta G]^2\rangle_m$ in the dependence of $\langle[\delta G]^2\rangle$ on the disorder strength Λ_0/v^2 was obtained, which clearly corresponds to the case (iii). For atomically-smooth disorder, a wide peak in the dependence of $\langle[\delta G]^2\rangle$ on Λ_0/v^2 with maximum $\langle[\delta G]^2\rangle_{\text{max}} \approx (4.5 - 5)\langle[\delta G]^2\rangle_m$ at $\Lambda_0/v^2 \sim 1$ was obtained. We believe this situation corresponds to the case (i), the maximum value being close to our prediction. We emphasize that our theory, just like that of Refs. [15, 16], requires *both* weak disorder ($\Lambda_0/v^2 \ll 1$) and the diffusive regime [$l = v/\gamma_0 \ll \mathcal{L} = \min(\mathcal{L}_x, \mathcal{L}_y)$]. The reason for having a peak, rather than a plateau, for smooth disorder in Ref. [14] is that the range of Λ_0/v^2 , where both these conditions are met, is quite narrow. The diffusive regime is not reached until disorder becomes strong ($\Lambda_0/v^2 \gtrsim 1$), while for smaller values of $\Lambda_0/v^2 \ll 1$ the system is simply in the ballistic regime $l \gtrsim \mathcal{L}$. This is supported by direct check of parameters ($l/\mathcal{L} \sim 0.1$ for $\Lambda_0/v^2 \sim 1$ and thus $l/\mathcal{L} \sim 1$ for $\Lambda_0/v^2 \sim 0.1$) and by an improving tendency (earlier upsurge of $\langle[\delta G]^2\rangle$ with increasing $\Lambda_0/v^2 \ll 1$) for larger samples (filled vs. open symbols).

Our theory thus helps understand the findings of Ref. [14] without assuming the existence of percolation paths and nonergodicity as was done by the authors. The ergodicity implies equivalence of averaging over disorder and the Fermi energy (or magnetic

field), $\langle f[G(\epsilon)] \rangle \doteq \lim_{\Delta\epsilon \rightarrow \infty} \frac{1}{\Delta\epsilon} \int_{\epsilon - \Delta\epsilon/2}^{\epsilon + \Delta\epsilon/2} d\epsilon' f[G(\epsilon')]$. For $f[G(\epsilon)] = G(\epsilon)$, this is clearly true, if $\mathcal{F}(\Delta\epsilon) \rightarrow 0$ as $\Delta\epsilon \rightarrow \infty$, see Eq. (11). This asymptotic of $\mathcal{F}(\Delta\epsilon)$ is determined by the behavior of the diffusion modes $D_{\Delta\epsilon}^i(\mathbf{q})$ at large energies $\Delta\epsilon$ and, in this respect, graphene is not any different from an ordinary metal [20]. One can estimate $\mathcal{F}(\Delta\epsilon) \propto \int_{\sqrt{\Delta\epsilon/D}}^{+\infty} q dq \frac{1}{q^4} \propto \frac{D}{\Delta\epsilon}$ for $\Delta\epsilon \gg \epsilon_x^*, \epsilon_y^*$. The proof for $f[G(\epsilon)] = [G(\epsilon)]^m$, $m > 1$, is analogous. Thus, the ergodic hypothesis for graphene holds. The violation of ergodicity in Ref. [14] occurred near the Anderson metal-insulator transition, and might be due to the fact that averaging over energy was mixing extended and localized states.

Conclusion. We have developed a theory of conductance fluctuations in monolayer graphene samples. We expect our findings presented in the *Results* section to be also completely applicable to bilayer graphene samples.

We thank SFB Transregio 12 for financial support.

-
- [1] K.S. Novoselov *et al.*, Nature **438**, 197 (2005); K. Novoselov *et al.*, Nature Physics **2**, 177 (2006).
 - [2] Y. Zhang *et al.*, Phys. Rev. Lett. **94**, 176803 (2005); Y. Zhang *et al.*, Nature **438**, 201 (2005).
 - [3] C. Berger *et al.*, J. Phys. Chem. B **108** 19912 (2004); J.S. Bunch *et al.*, Nano Lett. **5**, 287 (2005).
 - [4] C. Berger *et al.*, Science **312**, 1191 (2006).
 - [5] V.P. Gusynin and S.G. Sharapov, Phys. Rev. Lett. **95**, 146801 (2005); D. A. Abanin, P.A. Lee, and L.S. Levitov, Phys. Rev. Lett. **96**, 176803 (2006); J. Tworzydło *et al.*, Phys. Rev. Lett. **96**, 246802 (2006); V.V. Cheianov and V.I. Fal'ko, Phys. Rev. B **74**, 041403 (2006); M.I. Katnelson, Europhys. J. B **51**, 157 (2006), Europhys. J. B **52**, 151 (2006); I. L. Aleiner, D. E. Kharzeev, and A. M. Tsvelik, Phys. Rev. B **76**, 195415 (2007); V.V. Cheianov, V.I. Fal'ko, B.L. Altshuler, Science **315**, 1252 (2007).
 - [6] D. V. Khveshchenko, Phys. Rev. Lett. **97**, 036802 (2006).
 - [7] E. McCann *et al.*, Phys. Rev. Lett. **97**, 146805 (2006).
 - [8] A. F. Morpurgo and F. Guinea, Phys. Rev. Lett. **97**, 196804 (2006).
 - [9] I. L. Aleiner and K. B. Efetov, Phys. Rev. Lett. **97**, 236801 (2006).
 - [10] K. Kechedzhi *et al.*, Phys. Rev. Lett. **98**, 176806 (2007).
 - [11] S. V. Morozov *et al.*, Phys. Rev. Lett. **97**, 016801 (2006).
 - [12] H. B. Heersche *et al.*, Nature **446**, 56 (2007).
 - [13] R. V. Gorbachev *et al.*, Phys. Rev. Lett. **98**, 176805 (2007); arXiv:0708.1700; F. V. Tikhonenko *et al.*, arXiv:0707.0140.
 - [14] A. Rycerz, J. Tworzydło, and C.W.J. Beenakker, Europhys. Lett. **79**, 57003 (2007).
 - [15] B.L. Altshuler, JETP Lett. **41**, 648 (1985); B. L. Altshuler and D. E. Khmel'nitskii, JETP Lett. **42**, 359 (1985); B. L. Altshuler and B. I. Shklovskii, Sov. Phys. JETP **64**, 127 (1986).
 - [16] A.D. Stone, Phys. Rev. Lett. **54**, 2692 (1985); P.A. Lee and A.D. Stone, Phys. Rev. Lett. **55**, 1622 (1985).
 - [17] We are interested in the dependence on $\Delta\epsilon$ at *mesoscopic* scales set by the Thouless energy of the sample and there-

fore neglect $\Delta\epsilon$ compared to ϵ in quantities like the density of states ν , etc.

- [18] A.A. Abrikosov, L.P. Gorkov, and I.E. Dzyaloshinskii, *Methods of Quantum Field Theory in Statistical Physics*, Prentice Hall, New York (1963).
- [19] However, the density-density correlation function $P_\omega(\mathbf{r}, \mathbf{r}') = 2_s 2_v \nu [\delta(\mathbf{r} - \mathbf{r}') + i\omega D_\omega^0(\mathbf{r}, \mathbf{r}')]$, obtained from

Eq. (6), is expressed solely through the gapless mode D_ω^0 , as one would expect from the particle conservation law.

- [20] B.L. Altshuler, V.E. Kravtsov, and I.V. Lerner, *JETP Lett.* **43**, 441 (1986).